

**SURFACE DEFECT EVOLUTION IN HOT ROLLING OF HIGH SI-ELECTRICAL STEELS**

NIOI Manuel<sup>1</sup>, PINNA Christophe<sup>1</sup>, CELOTTO Steven<sup>2</sup>, SWART Edwin<sup>2</sup>, GHADBEIGI Hassan<sup>1</sup>

<sup>1</sup>*The University of Sheffield, Department of Mechanical Engineering, Sheffield, United Kingdom, EU,  
[mnioi1@sheffield.ac.uk](mailto:mnioi1@sheffield.ac.uk)*

<sup>2</sup>*Tata Steel Europe R&D, IJmuiden, The Netherlands, EU*

**Abstract**

Surface defects on metals products often have their root cause created during the hot rolling process by oxide scale in cavities and indents becoming embedded from the plastic deformation. The size and aspect ratio of these initial surface features are critical parameters determining whether they will be eliminated or not by the rolling process. The present research investigates the effects of initial defect geometry and the evolution mechanisms in the first hot rolling pass with the substrate being a high-silicon electrical steel. Laboratory hot-rolling experiments were carried out on blocks with open cavities of different geometries machined into the surface. The final geometry of the longitudinal and transversal profiles of the deformed defects were analysed from metallurgical cross-sections. The results were in good agreement with the literature, initial cavity dimensions was found to be crucial to determine whether the defect is eliminated or not after the rolling operation, in this case defects with a depth of 1 mm almost disappeared after the rolling. The results also show that for a given constant initial cavity width, the final defect width shows an inverse relationship with the selected initial depth. It has also been observed that at similar initial depth the wider defects evolve to much shallower surface features. The obtained results indicate that the length of the final defect is only dependent on its initial length along the rolling direction.

**Keywords:** Hot rolling, surface defect, electrical steel, deformation

**1. INTRODUCTION**

Hot rolling is among the key processes that is used to convert cast or semi-finished steel into finished products. The obtained surface integrity is of supreme importance specifically for thin sheets, such as those made by electrical steels, where no additional operations are used to modify the surface conditions. Electrical steels are usually produced with the gauge section in the order of 2-3 mm and they are usually used in the manufacture of electrical transformer cores. After casting, the slabs are continuously exposed to air at elevated temperatures up to 1250 °C [1], that results in oxide layers to be formed at different stages of the rolling which affects the roll bite tribology [2-7]. Although high pressure water spray is usually used to remove oxide scales [8, 9], the oxide scales can be entrapped in the surface imperfections with certain geometrical characteristics and/or aspect ratios. Slabs are rolled at several stages to reduce the thickness of the material to the final gauge. During this operation, initial protrusions and surface imperfections with embedded oxide scales are deformed and may conceal the oxide scale beneath the finished surface.

Several attempts have been made over the years to better understand generation and evolution mechanisms of surface defects in hot rolling processes [10-12]. C.J.Lee [10] studied evolution of artificial defects fabricated by drilling of cylindrical holes in the slabs subjected to multi-pass hot rolling experiments. They used several diameter to depth ratios to investigate effects of initial defect size on the final defect geometry. It was concluded that initial defects with diameter to depth ratios lower than 2 lead to severe defected surfaces. In a similar study M. J. Merwin [11] produced artificial imperfections on the surface of cast slabs to study the deformation behaviour during a full rolling process. It is reported that all the defects with initial depth of 20 mm and 30 mm were not eliminated during rolling, and the percentage of eliminated defects with depth of 10 mm and 5 mm were 67 % and 75 % respectively. Similar conclusions were reported in another study [12] where the

experimental results showed that the geometry of the initial defect is a critical factor on their elimination by further rolling steps.

In present research, the evolution of surface defects during hot rolling is studied for different initial defect aspect ratios for a 40 % thickness reduction. The initial and final geometry of the defects was parametrised to investigate the effects of initial geometry on the final defect shape, dimension and on the amount of oxide buried.

## 2. EXPERIMENTAL PROCEDURE

Electrical steel casting slabs with 3 % Si content were carefully selected from a roughing mill stand for this research. Six parts with a size of 115 x 85 x 25 mm were cut from the initial casting slabs provided. Cuboidal cavities with different dimensions (**Figure 1**) were machined into the top surface of the sections to resemble the surface defects prior to the rolling process. The dimensions of the machined defect in RD (length), TD (width) and ND (depth) directions were used as the control parameters in order to represent different aspect ratios of the defects.

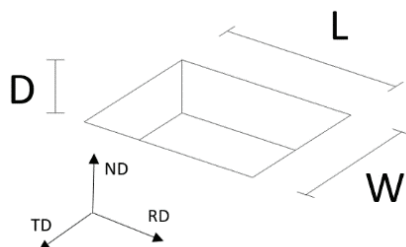


**Figure 1** Parameters used to describe the defect geometry

The control parameters (Depth, Length and Width) were varied at three values (levels) for detail analysis given access to the material and time required for the analysis. **Table** shows the defect list and the respective dimensions.

**Table 1** Control parameters dimensions

| D1 (mm) | D2 (mm) | D3 (mm) | L1 (mm) | L2 (mm) | L3 (mm) | W1 (mm) | W2 (mm) | W3 (mm) |
|---------|---------|---------|---------|---------|---------|---------|---------|---------|
| 1       | 3       | 5       | 4       | 10      | 17      | 3       | 7       | 11      |

The use of 3 levels for each factor will be useful to observe the interaction of the factors in different range levels, and to appreciate eventual quadratic relationships. The dimensions assigned at each level were carefully chosen to represent extreme conditions of the initial defects encountered in the industry.

**Figure 2** shows the machined defects using the 6 parts selected from the as cast material. The defects were machined such that the distance between adjacent cavities is large enough to prevent interaction of deformation fields between individual neighbouring defects. The defects are also located far from the lateral sides of the slab to ensure the lateral spreading of the material does not have any negative impact on the defects evolution mechanisms.

The slabs were rolled in a laboratory rolling mill with a 223 mm roll diameter. Slabs were heated at 1150 °C and held at this temperature for 15 minutes prior to the rolling process. This was to homogenise the internal temperature and to create a proper primary oxide scale in the surfaces. The slabs were then cooled to 1050 °C through radiation to the environment to simulate the heat loss in the hot rolling process after the slab came out of the furnace moving towards the first roughing mill. The oxide layer was removed by a scraper before the introduction of the slab into the rolling gap. The slab was then hot rolled at the velocity of 19 rpm with a reduction of 40 % achieved in a single rolling pass.



**Figure 2** Machined defects on the surface of slabs

After the rolling operation, the rolled surfaces of the slabs were analysed to identify the deformed defect geometries as well as the generated surface features. The final geometry of the longitudinal and transversal profiles of the deformed defects were analysed from metallurgical cross-sections to determine a relationship between the initial and deformed defect configurations and to identify the most critical defect geometries.

### 3. RESULTS

The defects have been visually inspected and the deformed geometry was characterised after the rolling operation. **Table 2** shows the comparison between the initial and deformed geometries of the selected defects. The rolling direction is vertical in all the images shown in the table. It is worth noting that all the defects were elongated along with the rolling direction. As can be seen, shallower defects disappeared (D1). Initial deeper defects appeared flattened but with a darker colour (D3) due to the impossibility to remove the oxide inside the holes with the scraping of the surface.

**Table 2** Optical photographs of the selected deformed defects on the surface of the rolled slabs

| D1 initial | D1 final | D2 initial | D2 final | D3 initial | D3 final |
|------------|----------|------------|----------|------------|----------|
|            |          |            |          |            |          |

The deformed lengths were measured directly from the top surface before the cutting, difference in oxide colours between defect and surface of the slab helped the identification of the defect final length. The depth and width of the deformed defects were measured from the micrographs of TD-ND sections, an average value of 5 measurements at various locations was considered to reduce the human interpretational errors. **Figure** shows a summary of the final depth, width and length measurement of the defects after rolling. The defects are elongated in the rolling direction (as visible from the first two rows of the table related to length), and reduced in width and depth, the initial 1 mm depth defects were mostly completely flattened.

| Defect number    | A1      | B1  | C1   | D1   | E1   | F1  | G1 | H1 | I1  | A2 | B2  | C2 | D2 | E2 | F2 | G2 | H2 | I2 | A3 | B3 | C3 | D3 | E3 | F3 | G3 | H3 | I3 |    |
|------------------|---------|-----|------|------|------|-----|----|----|-----|----|-----|----|----|----|----|----|----|----|----|----|----|----|----|----|----|----|----|----|
| Length<br>L (mm) |         |     |      |      |      |     |    |    |     |    |     |    |    |    |    |    |    |    |    |    |    |    |    |    |    |    |    |    |
|                  | final   |     |      |      |      |     |    |    |     |    |     |    |    |    |    |    |    |    |    |    |    |    |    |    |    |    |    |    |
| Width<br>W (mm)  |         |     |      |      |      |     |    |    |     |    |     |    |    |    |    |    |    |    |    |    |    |    |    |    |    |    |    |    |
|                  | initial |     |      |      |      |     |    |    |     |    |     |    |    |    |    |    |    |    |    |    |    |    |    |    |    |    |    |    |
| Depth<br>D (mm)  |         |     |      |      |      |     |    |    |     |    |     |    |    |    |    |    |    |    |    |    |    |    |    |    |    |    |    |    |
|                  | final   | 1   | 0.46 | 1    | 0.48 | 3   | 2  | 4  | 4.5 | 15 | 10  | 17 | 27 | 7  | 10 | 15 | 17 | 26 | 10 | 15 | 17 | 26 | 10 | 15 | 17 | 26 | 10 | 15 |
| initial          | 1       | 0.3 | 1    | 0.05 | 11   | 9.8 | 4  | 7  | 17  | 11 | 9.6 | 17 | 26 | 6  | 4  | 6  | 4  | 6  | 10 | 15 | 17 | 26 | 10 | 15 | 17 | 26 | 10 | 15 |

**Figure 3** Defect dimensions, before and after rolling

The micrographs of the selected defects (B3, G3) in the RD-ND and TD-ND planes taken from the midsection of the defects are shown in **Figure 4** and **Figure 5**, respectively. These are representing the typical deformation trend observed in the defects during rolling. The micrographs show material spreading in the transversal direction that results in a width reduction and buckling phenomenon in the side walls of the cavities (**Figure 4a**). Regarding the longitudinal direction, the front side shows an angle opening (**Figure 4c**), (**Figure 5a**), on the contrary the back surface is folded and closed leading to closing crevices sometimes (**Figure 4b**), this phenomena is caused by the rotation of the roll and the adhesion between slab and roll in the rolling gap.

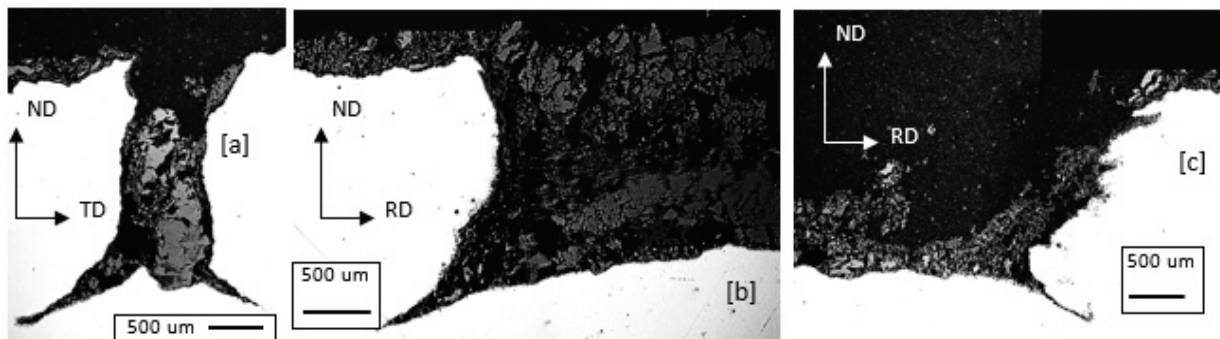


**Figure 4** Micrographs of B3 defect showing the deformed geometry at (a) the transverse section as well as (b, c) start and end part of the longitudinal section

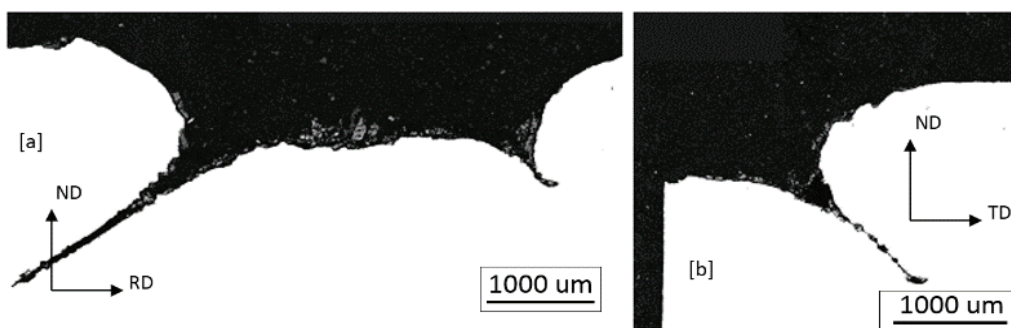


**Figure 5** Micrographs of G3 defect showing the deformed geometry at (a) the longitudinal section as well as (b) transverse section

#### 4. DISCUSSION

The results have revealed that if the rolling parameters including friction, thickness reduction, temperature field, etc. are constant, the final defect configuration is only dependent on the initial geometry including the aspect ratio of the cavities. It was found that the final length is not significantly affected by the initial width or depth of the defect as shown on (**Figure 3**). It is mostly related to the rolling procedure used such as reduction ratio, thus different initial width or depth could lead to similar final defect length. The width and depth of the deformed defects depend only on both initial depth and width, for a constant rolling procedure used. In this context, length does not have any significant effect on the final width and/or depths. The analysis of the micrographs in the transversal plane shows that defects with same initial widths show lower final width for higher initial depths. **Figure 6** shows an example of 2 different sections of defects where different initial depths and same initial widths are compared, it is noticeable that despite the defects had the same initial width, the deeper defect allowed the sides to spread transversally more than the shallower defect resulting in a narrower final defect..

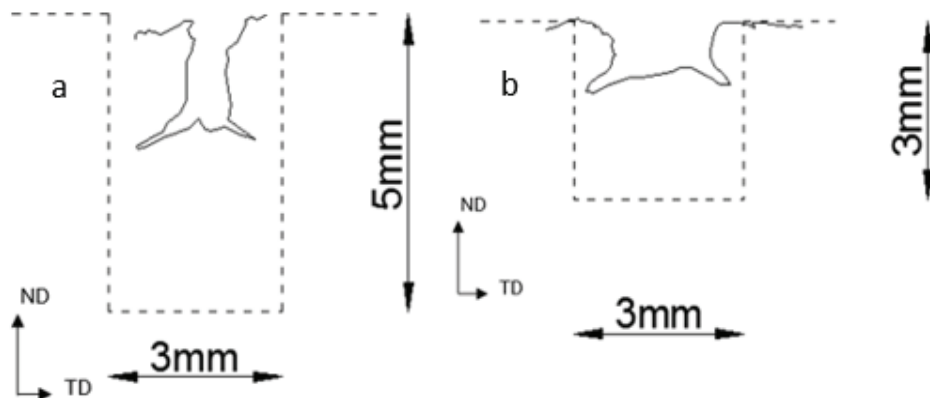


**Figure 6** Transversal section of the defects B3 (a), and B2 (b). The dash line represents the initial defect shape, the solid line represent the final defect section after the rolling.

It was also found that wider initial defects lead to shallower final defects for same initial depths. **Figure 7** shows an example of two different defects with same initial depth and different initial width. The comparison proves that despite both defects had same initial 5 mm depth, during the rolling the wider defect permitted the bottom surface to spread vertically because of the more space available, resulting in a shallower final defect.

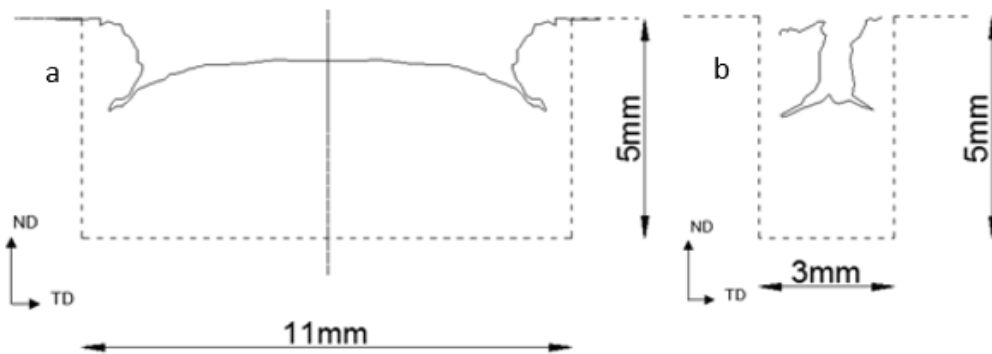


**Figure 7** Transversal section of the defects D3 (a), and B3 (b). The dash line represents the initial defect shape, the continuous line represent the final defect section after the rolling.

The **Figure 3** shows that complete flattening of the defect was obtained for shallower initial defects of 1 mm depth, and defects with an initial depth of 3 mm were almost flattened for wider defect cases only.

## 5. CONCLUSION

The results obtained from this study can be summarise as follows:

- All the defects were elongated and reduced in width and depth after the hot rolling procedure.
- The initial length of the defect doesn't play a crucial role in the generation of final defects.
- Due to the interaction between lateral sides and bottom surface of the defects, wider initial defects lead to shallower final defects, and on the contrary, deeper initial defects lead to narrower final defects.
- Initial defect depths lower than 1 mm are almost completely eliminated after the single rolling stand.

## ACKNOWLEDGEMENTS

***This project is financially supported by EPSRC Case studentship and Tata Steel EUROPE. Technical support of Tata Steel EUROPE is also greatly acknowledged.***

## REFERENCES

- [1] SONG, E.J., SUH, D.W., BHADESHIA, H.K.D.H., Oxidation of silicon containing steel. *Ironmak. Steelmak*, 1999, vol. 39, no. 8, pp. 599-604.
- [2] MUNTHER, P.A., LENARD, J.G., The effect of scaling on interfacial friction in hot rolling of steels, *Journal of material processing technology*, 1999, vol. 88, pp. 105-113.
- [3] LENARD, J.G., BARBULOVIC-NAD, L., The Coefficient of Friction During Hot Rolling of Low Carbon Steel, 2002, vol. 124, no. October, pp. 840-845.
- [4] KRZYZANOWSKI, M., BEYNON, J.H., FARRUGIA, D.C.J., *Oxide Scale Behaviour in High Temperature Metal Processing*, Wiley VCH, 2010.
- [5] HUM, B., COLQUHOUN, H.W., LENARD, J.G., Materials Processing Technology Measurements of friction during hot rolling of aluminum strips, 1996.
- [6] LENARD, J.G., An Experimental Study of Boundary Conditions in Hot and Cold Flat Rolling, no. 1, pp. 279-282, 1990.
- [7] LI, Y.H., SELLARS, C.M., Comparative investigations of interfacial heat transfer behaviour during hot forging and rolling of steel with oxide scale formation, 1998, vol. 81, pp. 282-286.
- [8] WANG, F., NING, L., ZHU, Q., LIN, J., DEAN, T.A., An investigation of descaling spray on microstructural evolution in hot rolling, 2008, pp. 38-47.
- [9] CHACKO, S., VASANI, S., RAY, A.K., Scale formation and its removal in Hot rolling Process, *Lechler Pvt. Ltd., Thane, India*.
- [10] LEE, C.J. S.L., Deformation analysis of surface defect on hot rolling by 3-D FEM simulation, *Rev. Metall. Cah. D'Informations Tech.*, 2008, vol. 105, no. 3, pp. 127-135.
- [11] MERWIN, M., Evolution of Artificially Induced Slab Imperfections Through Hot and Cold Rolling, *The Iron & Steel Technology Conference and Exposition*, Cleveland, Ohio, pp. 68-80, 2007.
- [12] SHAINU, S., ROY, T.K., DEY, B.K., SHARMA, R.K., GORAIN, N.C., DHAR, S., SASTRY, C.V., Study on Slab Surface Defects and Generation of FeO Type Slivers in Hot Rolled Coils, 2008, *Tata Steel Ltd. Jamshedpur*.